

Effects of Al_xGa_{1-x}N interlayer for GaN epilayer grown on Si substrate by metal-organic chemical-vapor deposition

Kung-Liang Lin, Edward-Yi Chang, Yu-Lin Hsiao, Wei-Ching Huang, Tien-Tung Luong, Yuen-Yee Wong, Tingkai Li, Doug Tweet, and Chen-Hao Chiang

Citation: *Journal of Vacuum Science & Technology B* **28**, 473 (2010); doi: 10.1116/1.3385672

View online: <http://dx.doi.org/10.1116/1.3385672>

View Table of Contents: <http://scitation.aip.org/content/avs/journal/jvstb/28/3?ver=pdfcov>

Published by the AVS: Science & Technology of Materials, Interfaces, and Processing

Articles you may be interested in

[Magnetostrictive effect in single crystal Fe_{1-x}Ga_x thin films](#)

J. Appl. Phys. **107**, 09A924 (2010); 10.1063/1.3367971

[Comparison of electrical properties and deep traps in p-Al_xGa_{1-x}N grown by molecular beam epitaxy and metal organic chemical vapor deposition](#)

J. Appl. Phys. **106**, 073706 (2009); 10.1063/1.3238508

[Semitransparent inverted polymer solar cells with MoO₃/Ag/MoO₃ as transparent electrode](#)

Appl. Phys. Lett. **95**, 053303 (2009); 10.1063/1.3196763

[Properties of single crystal Fe_{1-x}Ga_x thin films](#)

J. Appl. Phys. **105**, 07A938 (2009); 10.1063/1.3077207

[Growth of strained Si on high-quality relaxed Si_{1-x}Ge_x with an intermediate Si_{1-y}C_y layer](#)

J. Vac. Sci. Technol. A **23**, 1141 (2005); 10.1116/1.1913679



Re-register for Table of Content Alerts

Create a profile.



Sign up today!



Effects of $\text{Al}_x\text{Ga}_{1-x}\text{N}$ interlayer for GaN epilayer grown on Si substrate by metal-organic chemical-vapor deposition

Kung-Liang Lin, Edward-Yi Chang,^{a)} Yu-Lin Hsiao, Wei-Ching Huang, Tien-Tung Luong, and Yuen-Yee Wong

Department of Materials Science and Engineering, National Chiao Tung University, Hsinchu 300, Taiwan

Tingkai Li and Doug Tweet

SHARP Laboratories of America, Inc., Camas, Washington

Chen-Hao Chiang

Department of Electrophysics, National Chiao Tung University, 300, Taiwan

(Received 24 April 2009; accepted 15 March 2010; published 19 April 2010)

GaN film grown on Si substrate using multilayer AlN/ $\text{Al}_x\text{Ga}_{1-x}\text{N}$ buffer is studied by the low-pressure metal-organic chemical-vapor deposition method. The $\text{Al}_x\text{Ga}_{1-x}\text{N}$ films with Al composition varying from 1 to 0.66 were used to accommodate the stress induced between GaN and the Si substrate during GaN growth. The correlation of the Al composition in the $\text{Al}_x\text{Ga}_{1-x}\text{N}$ films with respect to the stress induced in the GaN film grown was studied using high-resolution x-ray diffraction, including symmetrical and asymmetrical $\omega/2\theta$ scans and reciprocal space maps. It is found that with proper design of the Al composition in the $\text{Al}_x\text{Ga}_{1-x}\text{N}$ buffer layer, crack-free GaN film can be successfully grown on 6 in. Si (111) substrates using multilayer AlN and $\text{Al}_x\text{Ga}_{1-x}\text{N}$ buffer layers. © 2010 American Vacuum Society. [DOI: 10.1116/1.3385672]

I. INTRODUCTION

Growth of GaN on Si (111) is of particular interest to the compound semiconductor industry due to lower cost and larger area, in comparison with other substrates and the possibility of integrating conventional Si-based devices with group III nitride devices on a single wafer. Due to the considerable differences in lattice parameters and thermal-expansion coefficients (CTEs) between GaN and Si substrates, the growth of high-quality, crack-free GaN films on a Si substrate poses serious difficulties. Thus, strain is an important issue for the growth of group III nitride growth on Si to achieve GaN-based devices, such as light-emitting diodes and field-effect transistors on a Si substrate. Therefore, a reduction in the stress and cracking in the GaN film is required for the growth of GaN on the Si (111) substrate. To obtain high-quality GaN film on Si substrates, the design of the interlayer structure between the GaN and the Si substrate is important. Using a low temperature AlN (LT-AlN) interlayer contributes to the reduction in the growth stress.¹⁻⁶ However, the quality of the AlN film grown at low temperature is inferior to the AlN grown at high temperature because of the formation of dislocations, especially the edge-threading dislocation (TD), at low temperatures, which influences the quality of the GaN film grown. On the other hand, due to the significant lattice mismatch between AlN and Si, cracks and higher defect density are formed on the AlN epilayer when it is grown at high temperature (1100 °C). Furthermore, compressive stress (about 9 GPa) is generated on GaN epitaxially grown on high-quality AlN due to the lattice mismatch between AlN and GaN.⁷ In this case, an $\text{Al}_x\text{Ga}_{1-x}\text{N}$ intermediate buffer should be used to reduce the lattice mis-

match between GaN and AlN.⁸ In this article, we report the properties of the GaN layer grown on a Si (111) substrate with a composite buffer, including a $\text{Al}_x\text{Ga}_{1-x}\text{N}$ interlayer with fixed Al composition (x was set at a fixed value between 0.5 and 0.25), a graded $\text{Al}_x\text{Ga}_{1-x}\text{N}$ layer (x varies from 1 to 0.66), and a multilayer AlN grown by the metal-organic chemical-vapor deposition (MOCVD) system. It is found that the composite buffer can greatly reduce the cracks and improve the crystal quality of the GaN layer grown and thus improve the structural and optical properties of the GaN layer.

II. EXPERIMENT

The multilayer AlN, the $\text{Al}_x\text{Ga}_{1-x}\text{N}$ layers, and the GaN film were grown by an EMCORE D-180 MOCVD reactor on a 6 -in. Si (111) wafer. The substrate resistivity, thickness, and warp were 7–13 Ω cm, 675 μm , and <30 μm , respectively. These wafers were Czochralski wafers with a single side polished. The trimethyl gallium (TMGa), trimethyl aluminum (TMAI), and ammonia (NH_3) were the source gases for Ga, Al, and N, respectively. H_2 was used as the carrier gas. The substrates were first degreased using a $\text{H}_2\text{SO}_4:\text{H}_2\text{O}_2:\text{H}_2\text{O}$ (3:1:1) solution for 5 min, then etched with HF (2%) for 1 min to remove the surface oxide layer before the epitaxial growth.⁹ After that, the Si (111) substrate was heated in the MOCVD reactor under H_2 ambient at 1050 °C for 10 min prior to growth to remove the surface oxide thermally. Before introducing NH_3 into the reactor, Al was predeposited for 10 s on Si substrate to prevent the formation of SiN_x . Figure 1 shows the layer structures of the samples grown in this study. As shown in Table I, sample A is a reference sample of GaN film grown on the Si (111) substrate with only a multilayer AlN buffer. The growth de-

^{a)}Electronic mail: edc@mail.nctu.edu.tw

GaN (1035 °C)
Fixed $\text{Al}_x\text{Ga}_{1-x}\text{N}$ (x : 0.25, 0.42, 0.5) 200 nm (1035 °C)
Graded $\text{Al}_x\text{Ga}_{1-x}\text{N}$ (x : 1~0.66) 500 nm (1035 °C)
HT-AIN 120 nm (1035 °C)
LT-AIN 50 nm (800 °C)
HT-AIN 30 nm (1035 °C)
150-mm Si (111) substrate

FIG. 1. Schematic view of GaN/Si(111) with the fixed $\text{Al}_x\text{Ga}_{1-x}\text{N}$ /graded $\text{Al}_x\text{Ga}_{1-x}\text{N}$ /HT-AIN/LT-AIN/HT-AIN buffer.

tails are as described in the earlier report.¹⁰ Samples B–D consist of a multilayer AIN combined with a graded $\text{Al}_x\text{Ga}_{1-x}\text{N}$ layer and a fixed $\text{Al}_x\text{Ga}_{1-x}\text{N}$ layer buffer. The GaN films were then grown on the top of these buffers. To control the Al fraction (x) in the fixed $\text{Al}_x\text{Ga}_{1-x}\text{N}$ interlayer, different TMGa flow rates of 16.6, 12.2, and 13.8 $\mu\text{mol}/\text{min}$ with fixed TMAI flow rate of 111.4 $\mu\text{mol}/\text{min}$ were used for samples B, C, and D, respectively. The growth time of the graded $\text{Al}_x\text{Ga}_{1-x}\text{N}$ and the fixed composition $\text{Al}_x\text{Ga}_{1-x}\text{N}$ layers was set at 40 and 20 min, respectively. The growth temperature of the multilayer AIN was 800 °C for the 50 nm LT-AIN layer and 1035 °C for the HT-AIN layers. Meanwhile, the growth temperature of the graded $\text{Al}_x\text{Ga}_{1-x}\text{N}$ layer, the fixed composition $\text{Al}_x\text{Ga}_{1-x}\text{N}$ layer, and the GaN layer were also set at 1035 °C. The reactor pressures were set at 50, 100, and 300 torr during the growth of the AIN, $\text{Al}_x\text{Ga}_{1-x}\text{N}$, and GaN layers, respectively. High-resolution x-ray diffractometry (XRD), transmission-electron microscopy (TEM), and an optical microscope were used to investigate the composition, structure, cross-sectional image, and the surface morphologies of the films. The stress states in the films were studied using the Raman spectroscopy.

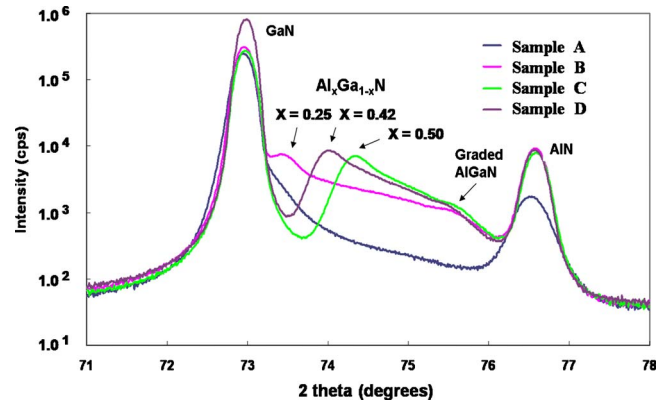


FIG. 2. (Color online) XRD ω - 2θ scan of GaN films grown on various types of multilayer AIN/graded $\text{Al}_x\text{Ga}_{1-x}\text{N}$ /fixed $\text{Al}_x\text{Ga}_{1-x}\text{N}$ composition buffers.

III. RESULTS AND DISCUSSION

Figure 2 shows the θ - 2θ XRD scans of the 0.8 μm GaN grown on different types of buffers with AIN multilayers in combination with a composition-graded $\text{Al}_x\text{Ga}_{1-x}\text{N}$ layer and a fixed Al composition $\text{Al}_x\text{Ga}_{1-x}\text{N}$ layer. The detailed buffer structures of samples A–D are as listed in Table I and Fig. 1. In this case, the thicknesses of the graded $\text{Al}_x\text{Ga}_{1-x}\text{N}$ layer and the fixed composition $\text{Al}_x\text{Ga}_{1-x}\text{N}$ layer are 500 and 200 nm, respectively. The Al composition in the $\text{Al}_x\text{Ga}_{1-x}\text{N}$ layers was determined from the lattice constant measurement using XRD, assuming that Vegard's law is obeyed by the $\text{Al}_x\text{Ga}_{1-x}\text{N}$ films. Figure 2 presents the variation in the XRD 2θ scan for the $\text{Al}_x\text{Ga}_{1-x}\text{N}$ film with Al composition varying from 0.5 to 0.25. The rocking curves of the GaN (004) and AIN (004) plans were also scanned for each sample. The full width at half maximum (FWHM) values of the rocking curves are listed in Table I. For sample D, the FWHMs of the GaN (004) and AIN (004) scans are the smallest. As the Al mole fraction (x) of the fixed composition $\text{Al}_x\text{Ga}_{1-x}\text{N}$ increases from 0.25 to 0.42, the crystal quality of GaN also improves due to the reduction in the lattice mismatch between GaN and AIN. However, when Al mole fraction is higher than 0.42, the crystallinity of GaN becomes worse. This is because of a considerable amount of misfit strain has been induced due to the large differences in CTE and lattice constant, when the Al concentration is higher than 0.42. This result is in agreement with the reports by Raghavan and Redwing¹¹ and Saengkaew *et al.*¹² Therefore, it can be con-

TABLE I. Layer thickness, composition, and induced strain for samples A–D with different buffers.

Sample	GaN thickness (μm)	AIN ^a thickness (nm)	Graded $\text{Al}_x\text{Ga}_{1-x}\text{N}$ thickness (nm)	Fixed $\text{Al}_x\text{Ga}_{1-x}\text{N}$ x fraction	Fixed $\text{Al}_x\text{Ga}_{1-x}\text{N}$ thickness (nm)	AIN strain (ϵ_a)	AIN XRD (004) FWHM (deg)	GaN strain (ϵ_a)	GaN XRD (004) FWHM (deg)
A	0.8	200	0	0	0	0.378	0.717	0.146	0.322
B	0.8	200	500	0.25	200	0.335	0.319	0.137	0.228
C	0.8	200	500	0.50	200	0.312	0.357	0.132	0.242
D	0.8	200	500	0.42	200	0.300	0.293	0.120	0.158

^aMultilayer AIN (high temperature/low temperature/high temperature AIN).

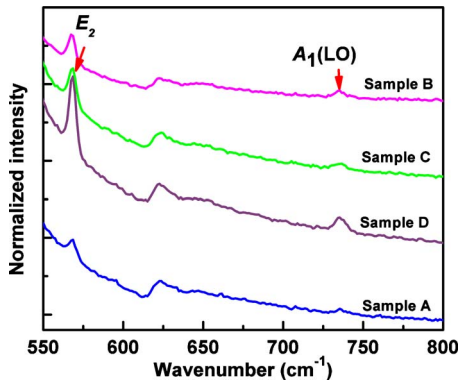


Fig. 3. (Color online) Raman spectrum of samples with GaN films grown on different buffer structures.

cluded that with the Al mole fraction $x=0.42$ in the fixed $\text{Al}_x\text{Ga}_{1-x}\text{N}$ film, the strain induced by the lattice mismatch between $\text{Al}_x\text{Ga}_{1-x}\text{N}$ and other films compensates the strains induced in the GaN and AlN films on the Si substrate.

The thermal stress ε can be calculated from the average value of the CTE of Si and GaN using the following relation:¹³ $\varepsilon = (\alpha_{\text{GaN}} - \alpha_{\text{Si}})(T_{\text{growth}} - T_{\text{RT}})$, where α_{GaN} and α_{Si} are the CTEs of GaN ($5.59 \times 10^{-6} \text{ K}^{-1}$) and Si ($3.59 \times 10^{-6} \text{ K}^{-1}$), respectively. T_{growth} and T_{RT} are the growth temperature (1035 °C) and room temperature (25 °C), respectively. The tensile strain of GaN grown on Si after cooling down was $\varepsilon=0.202\%$. Table I shows that the strain in the GaN film is smaller than the theoretical nature tensile. This means that AlN and $\text{Al}_x\text{Ga}_{1-x}\text{N}$ interlayers can reduce the thermal stress induced during the cooling effectively.

Since the Al composition in the $\text{Al}_x\text{Ga}_{1-x}\text{N}$ layers could be accurately controlled by the MOCVD growth, a graded $\text{Al}_x\text{Ga}_{1-x}\text{N}$ interlayer with a total thickness of about 500 nm was successfully grown on top of the AlN buffer layer to reduce the lattice strain further and improve the GaN properties. Figure 2 shows the 2θ XRD scan of the GaN films grown on the multilayer AlN buffer with a graded $\text{Al}_x\text{Ga}_{1-x}\text{N}$ interlayer in the samples. As the Al composition in the $\text{Al}_x\text{Ga}_{1-x}\text{N}$ interlayer was graded, the thermal-expansion coefficient of the graded $\text{Al}_x\text{Ga}_{1-x}\text{N}$ interlayer was gradually changed from that of AlN to that of GaN. Therefore, the thermal stress may be accommodated within the graded $\text{Al}_x\text{Ga}_{1-x}\text{N}$ interlayer. It is expected that a complete elimination of cracks can be achieved through optimization of the composition and thickness of the graded $\text{Al}_x\text{Ga}_{1-x}\text{N}$ interlayer.

The room-temperature Raman spectra of the E_2 -high and A_1 (LO) line for the samples are presented in Fig. 3. The spectra show strong E_2 (TO)-high and A_1 (TO) modes under $z(x_-)z$ scattering geometry. The E_2 (TO) Raman peak is generally used to estimate the in-plane strain. For samples A–D, the Raman shifts of the E_2 (TO) phonon peaks were 566.8, 566.6, 566.9, and 567.2 cm^{-1} , respectively. The residual stresses in the samples were calculated from the measured wave number shifts of the E_2 -high mode in the Raman spectra.¹⁴ The values of the tensile stress in the GaN films

(sample A is 0.162 GPa, sample B is 0.209 GPa, sample C is 0.139 GPa, and sample D is 0.069 GPa) were calculated using the E_2 phonon peak observed at 567.5 cm^{-1} for a 400- μm -thick, freestanding, and strain-free GaN and the relation $\Delta\omega = K\sigma_{xx} \text{ cm}^{-1} \text{ GPa}^{-1}$. Here $\Delta\omega$ is the phonon peak shift, σ is the biaxial stress, and $K=4.3$ is the pressure coefficient.¹⁵ Sample D shows a significant reduction in the in-plane stress, as compared to samples A–C. The stress in sample D is also smaller than the stress values reported recently for different buffer schemes.^{16–18} Comparing the stress and the Raman shift, a direct relationship between biaxial stress and phonon shift in GaN/Si(111) can be derived.

The surfaces of all samples grown were mirrorlike. However, crack lines were found near the wafer edges on samples A–C as observed by optical microscope. Meanwhile, sample D was crack-free, the optical micrograph showing crack-free GaN on Si was reported in an earlier report.¹⁰ In this study, the insertion of a graded composition $\text{Al}_x\text{Ga}_{1-x}\text{N}$ interlayer and a fixed composition $\text{Al}_{0.42}\text{Ga}_{0.58}\text{N}$ layer has significantly compensated the tensile stress induced in the GaN film grown on Si substrate. The reduction in in-plane tensile stress was further evidenced by the improved crystalline quality of the GaN films in sample D, for which the GaN (004) FWHM was only 0.158 arc sec. In sample D, the wafer bowing was $-8.63 \mu\text{m}$ and the radius of curvature was 238.96 m. Photoluminescence mapping was used to evaluate the film quality and film uniformity. The peak wavelength distribution was quite narrow, ranging from 364.5 to 367 nm. The mean value was 365.3 nm with standard deviation of 0.2%.

A second source of stress is the lattice mismatch between the buffer and the GaN film. It can be evaluated by measuring an asymmetric reflection plane using reciprocal space mapping (RSM). RSM mapping was used to measure the a -axis lattice constants (a_{film}) of the AlN, AlGa_N, and GaN layers grown. The data were compared to the a -axis lattice constants (a_{bulk}) of bulk AlN, AlGa_N, and GaN materials in order to calculate the strains. If the $a_{\text{film}} > a_{\text{bulk}}$, the film is in tensile stress. If the $a_{\text{film}} < a_{\text{bulk}}$, the film is in compressive stress. The strains can be calculated using the following relationship:

$$\varepsilon_a = [(a_{\text{film}} - a_{\text{bulk}})/a_{\text{bulk}}] \times 100\%.$$

Figure 4 shows the (10-15) RSM of sample D. The epilayer structure of sample D consists of the top GaN layer, a fixed $\text{Al}_{0.42}\text{Ga}_{0.58}\text{N}$ layer, a graded $\text{Al}_x\text{Ga}_{1-x}\text{N}$ (x from 1 to 0.66) layer, and the multilayer AlN buffer on the bottom. The average lattice constants of GaN and AlN films obtained were $a_{\text{film}}^{\text{GaN}} = 3.1928 \text{ \AA}$ and $a_{\text{film}}^{\text{AlN}} = 3.1203 \text{ \AA}$, respectively. As compared to the bulk of GaN and AlN lattice constant values ($a_{\text{bulk}}^{\text{GaN}} = 3.189 \text{ \AA}$ and $a_{\text{bulk}}^{\text{AlN}} = 3.111 \text{ \AA}$), it is obvious that the GaN and AlN were not fully relaxed (in-plane strain $\varepsilon_{a,\text{GaN}} = 0.12\%$ and $\varepsilon_{a,\text{AlN}} = 0.3\%$). In this figure, the AlN reciprocal-lattice points are distributed on top of the solid line boxed region, which means that the AlN multilayer is under tensile strain (ε_a) of about 0.3%. The GaN reciprocal-lattice points are distributed at the bottom of the solid line boxed region,

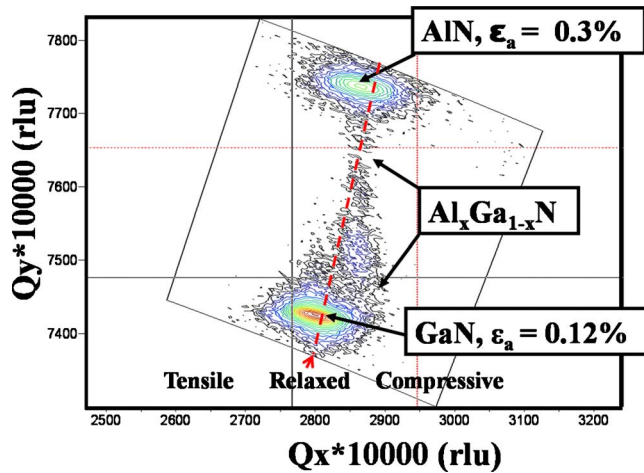


FIG. 4. (Color online) Reciprocal space mapping of sample D for GaN on Si (111) with multilayer AlN and graded $\text{Al}_x\text{Ga}_{1-x}\text{N}$ buffer.

which indicates that the GaN film is under small tensile strain (ϵ_a) of about 0.12%. The graded $\text{Al}_{0.66}\text{Ga}_{0.34}\text{N}$ and fixed $\text{Al}_{0.42}\text{Ga}_{0.58}\text{N}$ reciprocal-lattice points are distributed between AlN and GaN reciprocal-lattice points. These $\text{Al}_x\text{Ga}_{1-x}\text{N}$ reciprocal-lattice points were located at the side of the “relaxed” line, showing that they are in compressive stress. It is believed that this $\text{Al}_x\text{Ga}_{1-x}\text{N}$ layer helped compensate the tensile stress formed in the AlN buffer and resulted in the crack-free GaN film on Si.

Usually three types of dislocations are present in the GaN, namely, screw, edge, and mixed dislocations, with Burgers vector $\mathbf{b}=[0001]$, $\mathbf{b}=1/3 [11-20]$, and $\mathbf{b}=1/3 [11-23]$, respectively. By using two-beam conditions for two perpendicular diffraction vectors $\mathbf{g}=[0002]$ and $\mathbf{g}=[1-100]$ and the invisibility criteria $\mathbf{g}\cdot\mathbf{b}=0$, screw and edge dislocations can be observed using a TEM. Figures 5(a) and 5(b) give two-beam cross-sectional TEM images of sample D with diffraction vector along $\mathbf{g}=[0002]$ and $\mathbf{g}=[1-100]$ to determine screw and edge TDs, respectively. The graded $\text{Al}_x\text{Ga}_{1-x}\text{N}$ interfaces can be seen clearly. As shown in Fig. 5(a), it is found that the screw-dislocation density (SDD) at the bottom of graded $\text{Al}_x\text{Ga}_{1-x}\text{N}$ is over 10^{10} cm^{-2} . The dislocation density decreases gradually as the film thickness of the $\text{Al}_x\text{Ga}_{1-x}\text{N}$ interlayer increases. The SDDs at the top of GaN layer reduce to $4.1 \times 10^8 \text{ cm}^{-2}$. In addition, as can be seen from Fig. 5(b), the number of edge dislocations threading through the interface between graded $\text{Al}_x\text{Ga}_{1-x}\text{N}$ and GaN to the top GaN layer is greatly reduced. The edge-dislocation density (EDD) for this sample is estimated to be over 10^9 cm^{-2} at the bottom of the graded $\text{Al}_x\text{Ga}_{1-x}\text{N}$ layer, while it reduces to $2.7 \times 10^8 \text{ cm}^{-2}$ at the GaN region on the top. For comparison, the SDDs and EDDs in sample A are 5.7×10^9 and $4.3 \times 10^9 \text{ cm}^{-2}$, respectively (not show here). The Al fraction in the $\text{Al}_x\text{Ga}_{1-x}\text{N}$ gradually decreased from 1 to 0.66. The graded $\text{Al}_x\text{Ga}_{1-x}\text{N}$ interlayer may have bent the propagation direction of the edge TD during the film growth. The bending of the edge TDs would enhance the recombination and annihilation of the TDs. After inserting the fixed

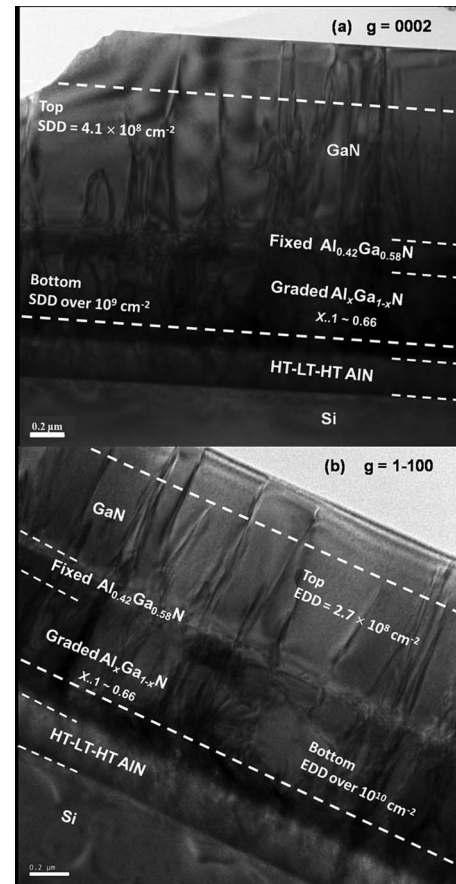


FIG. 5. Cross-sectional TEM images of sample D (a) with diffraction vector $\mathbf{g}=[0002]$ and (b) with diffraction vector $\mathbf{g}=[1-100]$.

$\text{Al}_{0.42}\text{Ga}_{0.58}\text{N}$ layer, the number of edge TDs was gradually reduced due to further bending and annihilation on the edge TDs, as shown in Fig. 5(b). The driving force for the increased dislocation annihilation within the graded layer was the built-in gradient of the strain, which was caused by the gradient of the composition. This leads to an increased bending of dislocations into the growth plane, where they can annihilate efficiently and improve the quality of the GaN film. Moreover, the bending of edge TDs not only increased the annihilation of the edge TD but also reduced the film stress of the GaN layer, as was also observed by Wong *et al.*¹⁹ As shown in Fig. 5(a), the screw TDs were also greatly reduced in the GaN film. The screw TDs may not be reduced by the bending mechanism because their Burgers vectors are parallel with each other in the growth direction. The reduction in screw TDs in the GaN layer was due to the blocking of their growth by the fixed $\text{Al}_{0.42}\text{Ga}_{0.58}\text{N}$ interlayer. The result suggests that $\text{Al}_{0.42}\text{Ga}_{0.58}\text{N}$ film is sufficient to block the propagation of the screw TDs. Higher Al content of $\text{Al}_x\text{Ga}_{1-x}\text{N}$ could generate new TDs due to larger lattice mismatch between the $\text{Al}_x\text{Ga}_{1-x}\text{N}$ and GaN films.

IV. CONCLUSIONS

A multilayer AlN film structure combined with $\text{Al}_x\text{Ga}_{1-x}\text{N}$ films was used as the composite buffer to reduce the tensile

stress of the GaN film grown on the Si (111) substrate. Two types of $\text{Al}_x\text{Ga}_{1-x}\text{N}$ layers, one with graded Al concentration and the other with fixed Al concentration, were incorporated into the buffer. The correlation between the Al composition in the $\text{Al}_x\text{Ga}_{1-x}\text{N}$ layer and the stress induced in the GaN film grown was studied. It is found that with a graded $\text{Al}_x\text{Ga}_{1-x}\text{N}$ layer (x varies from 1 to 0.66) and a fixed $\text{Al}_{0.42}\text{Ga}_{0.58}\text{N}$ interlayer incorporated in the AlN based buffer, the tensile stress in the GaN film can be significantly reduced to 0.069 GPa. This leads to the successful deposition of crack-free GaN film on the 6-in. Si (111) substrate. Using this composite buffer layers, the crystal quality of the GaN grown on Si substrate was also significantly improved.

ACKNOWLEDGMENTS

The authors would like to acknowledge the assistance and support of the National Science Council and the Ministry of Economic Affairs, Taiwan under Contract No. NSC 97-2221-E-009-156-MY2.

¹T. Takeuchi, H. Amano, K. Hiramatsu, N. Sawaki, and I. Akasaki, *J. Cryst. Growth* **115**, 634 (1991).

²A. Strittmatter, A. Krost, M. Straßburg, V. Türck, D. Bimberg, J. Bläsing,

and J. Christen, *Appl. Phys. Lett.* **74**, 1242 (1999).

³Y. Nakada, I. Aksenov, and H. Okumura, *Appl. Phys. Lett.* **73**, 827 (1998).

⁴S. Guha and N. A. Bojarczuk, *Appl. Phys. Lett.* **73**, 1487 (1998).

⁵C. A. Tran, A. Osinski, R. F. Karlicek, and I. Berishev, *Appl. Phys. Lett.* **75**, 1494 (1999).

⁶J. W. Yang, A. Lunev, G. Simin, A. Chitnis, M. Shatalov, M. A. Khan, J. E. Van Nostrand, and R. Gaska, *Appl. Phys. Lett.* **76**, 273 (2000).

⁷S. Zamir, B. Meyler, and J. Salzman, *Appl. Phys. Lett.* **78**, 288 (2001).

⁸A. Dadgar, J. Bläsing, A. Alam, M. Heuken, and A. Krost, *Jpn. J. Appl. Phys., Part 2* **39**, L1183 (2000).

⁹E. V. Etzkorn and D. R. Clarke, *J. Appl. Phys.* **89**, 1025 (2001).

¹⁰K. L. Lin *et al.*, *Appl. Phys. Lett.* **91**, 222111 (2007).

¹¹S. Raghavan and J. Redwing, *J. Appl. Phys.* **98**, 023515 (2005).

¹²P. Saengkaew, A. Dagar, J. Bläsing, T. Hempel, P. Veit, J. Christen, and A. Krost, *J. Cryst. Growth* **311**, 3742 (2009).

¹³G. A. Slack and S. F. Bartram, *J. Appl. Phys.* **46**, 89 (1975).

¹⁴S. Tripathy, S. J. Chua, P. Chen, and Z. L. Miao, *J. Appl. Phys.* **92**, 3503 (2002).

¹⁵S. Guha, R. C. Keller, V. Yang, F. Shahedipour, and B. W. Wessels, *Appl. Phys. Lett.* **78**, 58 (2001).

¹⁶K. Koh, Y. J. Park, E. K. Kim, C. S. Park, S. H. Lee, J. H. Lee, and S. H. Choh, *J. Cryst. Growth* **218**, 214 (2000).

¹⁷L. S. Wang, K. Y. Zang, S. Tripathy, and S. J. Chua, *Appl. Phys. Lett.* **85**, 5881 (2004).

¹⁸M. Jamil, J. R. Grandusky, V. Jindal, F. Shahedipour-Sandvik, S. Guha, and M. Arif, *Appl. Phys. Lett.* **87**, 082103 (2005).

¹⁹Y. Y. Wong, E. Y. Chang, T. H. Yang, J. R. Chang, Y. C. Chen, J. T. Ku, C. T. Lee, and C. W. Chang, *J. Cryst. Growth* **311**, 1487 (2009).